

Modeling of Impurity Radiation and Transport during Long Pulse 'Breathing' Plasmas in LHD

PETERSON Byron J.*, RICE John E.¹, YAMAZAKI Kozo, NAKAMURA Yukio, NODA Nobuaki, TAKEIRI Yasuhiko, GOTO Motoshi, IDA Katsumi, NARIHARA Kazumichi, TANAKA Kenji, SATO Kuninori, SHOJI Mamoru, MASUZAKI Suguru, SAKAKIBARA Satoru, OSAKABE Masaki, FUNABA Hisamichi, OKA Yoshihide, KANEKO Osamu, TSUMORI Katsuyoshi, SATO Motoyasu, SHIMOZUMA Takashi, KAWAHATA Kazuo, OHYABU Nobuyoshi, SUDO Shigeru and MOTOJIMA Osamu
National Institute for Fusion Science, Toki-shi, 509-5292, JAPAN

¹*Plasma Science & Fusion Center, Mass. Inst. of Tech., Cambridge, MA 02139-4294, USA*

(Received: 18 January 2000 / Accepted: 15 May 2000)

Abstract

During long pulse plasmas with a stainless steel divertor in the Large Helical Device (LHD) a slow oscillation ($t = 1.5$ s) known as the 'Breathing' Plasma has been observed. Expansion and contraction observed in the CCD video images are from changes in the radiating volume of the light impurities due to fluctuations of the edge electron temperature. Modeling of the radiation shows that the core iron density varies by a factor of three while carbon and oxygen densities remain constant.

Keywords:

LHD, long pulse, impurity transport, radiation

1. Introduction

Impurity accumulation is an important issue for the steady state operation of fusion devices as it can lead to increased radiation and premature termination of the discharge through radiative collapse as well as dilution of the fueling gas. Evidence of this has been observed in tokamaks, particularly in the high confinement regime [1]. Heavy impurities in particular have the ability to radiate at higher temperatures and therefore can cool the core plasma [2]. The effect of lighter impurities is limited to the edge plasma and therefore is less detrimental to the plasma performance. This was seen in the Heliotron-E stellarator through the effect of a carbon limiter on the reduction of metallic impurities [3]. In this paper we model the impurity radiation and transport in LHD [4] during a long pulse discharge where a slow oscillation known as the 'breathing' plasma is observed

[5]. In doing so we aim to learn about the role that impurities are playing in this oscillation.

During the second experimental cycle of LHD an oscillation in the major plasma bulk parameters was observed during long-pulse neutral-beam operation which is known as the 'breathing' plasma. An example of the electron temperature profiles, line-averaged density, total radiated power and light impurity line radiation signals during a 'breathing' plasma oscillation having a period of about 1.5 seconds is shown in Fig. 1. One striking feature of this oscillation is the relationship between the density, the total radiated power and the spectroscopic signals of the light impurities during the rising phase of the density. In a typical LHD discharge the radiated power rises with the line averaged density until a density limit is reached and the plasma collapses

*Corresponding author's e-mail: peterson@LHD.nifs.ac.jp

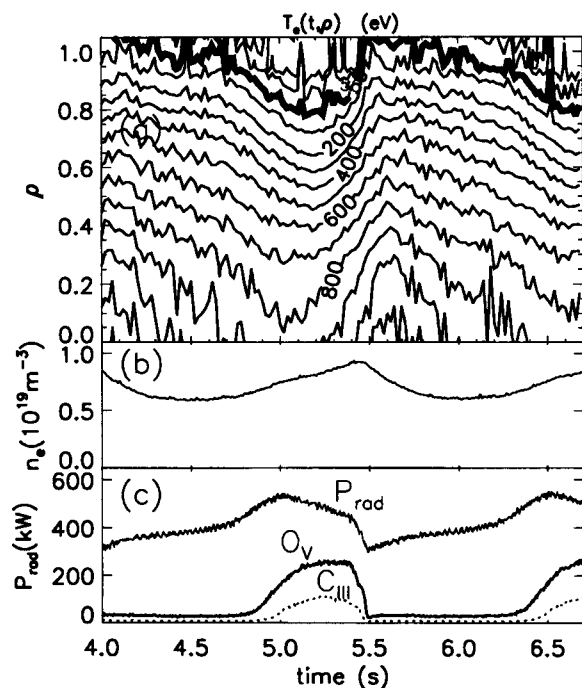


Fig. 1 Time histories for shot 6690 of (a) electron temperature profiles, (b) line-averaged density, (c) total radiated power, C_{III} and O_V .

radiatively [6]. However, in the 'breathing' plasma, during the rising phase of the density the total radiated power is seen to rise initially reaching a peak and then to decrease while the density continues to rise. Meanwhile as the total radiated power decreases the line radiation from the light impurities, carbon and oxygen, increases sharply. This suggests two things. First of all the decrease in the total radiated power as the radiation from light impurities increases indicates that iron, the other intrinsic impurity, is strongly contributing to the total radiated power. Secondly the decrease in the radiated power as the density increases indicates that the radiation from iron is decreasing rapidly due to either a change in the electron temperature decreasing the cooling rate or a decrease in the impurity density. In this paper, using profile data from bolometer arrays for radiated power, UV line radiation measurements of the light impurities, visible CCD video images, Thomson scattering for electron temperature and FIR interferometer for density, we investigate the roles that impurities may be playing in this oscillation.

2. Cooling Rates for Impurities from ADPAK

In order to understand the relative role that impurities are playing in the plasma it is instructive to

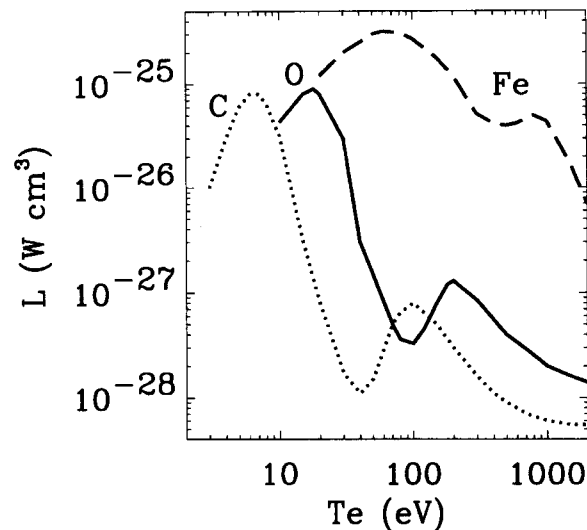


Fig. 2 Cooling rates vs T_e from ADPAK for carbon, oxygen and iron.

examine the cooling rates, L_Z , as a function of the electron temperature, T_e , based on the average ion model, assuming coronal equilibrium [7]. These are shown in Fig. 2 for the intrinsic impurities, carbon, oxygen and iron. The impurity emissivity, S_Z , can be calculated from L_Z , T_e , the impurity density, n_Z , and the electron density, n_e , using

$$S_Z = n_Z n_e L_Z(T_e). \quad (1)$$

From looking at the cooling rates one can see that carbon peaks at 6 eV, oxygen at 20 eV and iron dominates over the other two impurities for electron temperatures greater than 50 eV.

3. Behavior of Carbon and Oxygen

The first observations of the 'breathing' plasma appeared in the real-time CCD images which showed a pulsation in the visible radiation with a period of 1.5 s. This observation led to the name 'breathing'. The video signal can be divided into two phases. In one phase (Fig. 3a) the visible radiating region is seen to broaden and contract in minor radius while brightening. In the other phase (Fig. 3b) the radiating region narrows and expands in minor radius while becoming dimmer. Examination of the electron temperature profile evolution shown in Fig. 1 can give a better understanding of the video images. At $t = 5.25$ s (corresponds to Fig. 3a) the electron temperature is at a minimum. The drop in the electron temperature at the edge results in the minor radially inward motion and

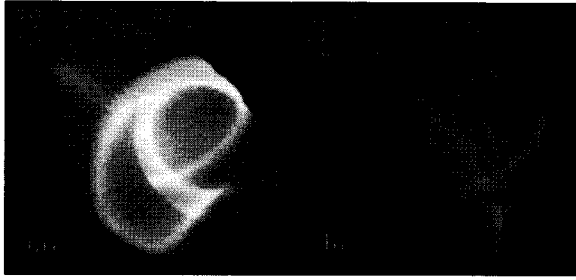


Fig. 3 Tangentially viewing CCD video image of shot 6690 at $t =$ (a) 5.25 s and (b) 5.75 s.

broadening of the radiating region for light impurities which corresponds to the area above the thick 50 eV contour in Fig. 1a. This explains the peak in the light impurity signals in Fig. 1c and the image seen in Fig. 3a as described earlier. During this period the electron density is growing which also contributes to the increase in radiation. At $t = 5.75$ s (corresponds to Fig. 3b) the electron temperature is near its maximum as seen in Fig. 1a. This results in the radiating region for light impurities becoming smaller and moving to the low-density region outside the last closed flux surface in agreement with the image seen in Fig. 3b. The consequent reduction in the radiation from light impurities is evident in Fig. 1c.

In order to determine what role the carbon and oxygen impurity densities may be playing in this oscillation we have modeled the C_{III} and O_V signals. This modeling was carried out using the MIST [8] transport code to determine the charge state density profiles from the electron density and temperature profiles and assuming a spatially invariant diffusion coefficient of $0.2 \text{ m}^2/\text{s}$ and no inward convection ($v = 0.0 \text{ m/s}$). The emissivity profiles for the transitions in question can then be calculated using the collisional-radiative model of the LINES [9] code which are then integrated along the line of sight to give the brightness time histories. The results of this modeling are shown with the measured lines in Fig. 4. It was assumed that both the diffusion coefficient and the total impurity densities were constant in time. The agreement between the measured and calculated brightness histories indicates that both of these assumptions are correct to within the errors of the measurements. This means that the change in the brightness of the light impurities during the oscillation is due mainly to the change in the electron temperature and density and not due to large changes in the impurity density and transport.

Besides these data from the ultraviolet, visible

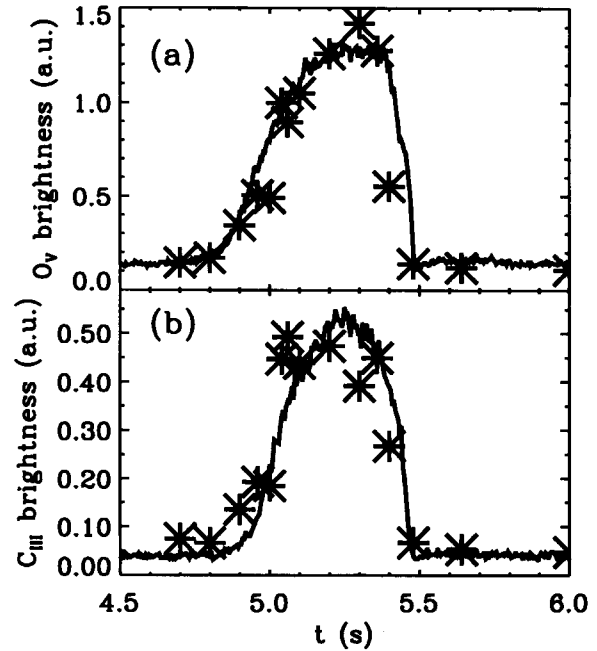


Fig. 4 Line radiation brightness from shot 6690 for (a) O_V and (b) C_{III} with transport model (*).

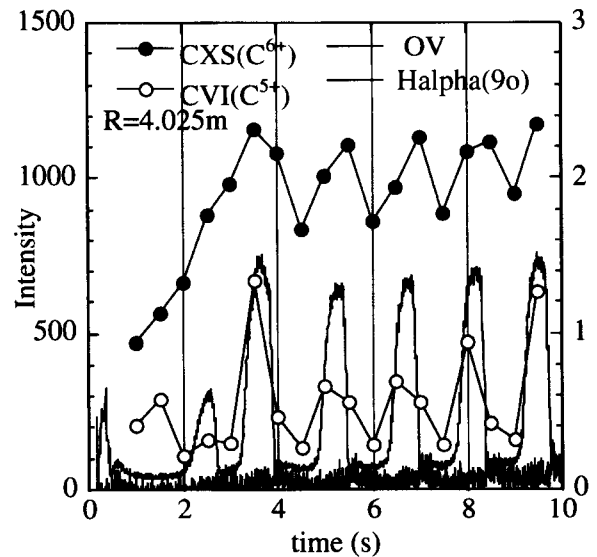


Fig. 5 Line radiation brightness from shot 6690 for C^{6+} and C^{5+} at $R = 4.025 \text{ m}$ and O_V and H_{α} .

emission from fully ionized carbon (C^{6+}) shows that there is only about a 20% change in the carbon density, as seen in Fig. 5. On the other hand, C^{5+} , which has a dependence on the electron temperature, shows a much larger variation similar to that seen in O_V and C_{III} .

4. Behavior of Iron Impurity

While carbon and oxygen should radiate from the low temperature edge plasma, iron should dominate the radiation inside $r = 0.8$ where $T_e > 50$ eV. Therefore we can calculate the iron density profile evolution for this region from the measured radiated power, electron density and temperature profiles and the iron cooling rate from Fig. 2 using Eq. 1. The result of this calculation at $r = 0.4$ is shown in Fig. 6. One notes in contrast to the light impurities that the iron density is strongly oscillating in time, varying by a factor of 3 in amplitude. The oscillation in the emissivity at this radius can be nearly completely attributed to the oscillation in the iron density as the electron density is oscillating out of phase and the temperature dependence of the iron cooling rate at this temperature range is weak. The time derivative of the electron temperature is well correlated with the amplitude of the iron density indicating that radiation from iron is cooling the plasma at this radius.

Additional data from the vacuum ultraviolet region for a similar shot show radiation from iron oscillating out of phase with that from the lighter impurities as seen in Fig. 7. This is in agreement with the phasing of the radiation at $\rho = 0.4$ shown in Fig. 6 compared with the phasing of the lighter impurities shown in Fig. 1. Also, similar oscillations have been observed in spectroscopic signals from F_{eXVI} [10].

5. Conclusions and Discussion

The expansion and contraction evident in the video images of 'breathing' plasma are due to the motion and the change in size of the radiating volume for light impurities resulting from the rise and fall of the edge electron temperature. However, transport analysis of the light impurities shows that their densities are not changing significantly during the oscillation. On the other hand, calculation of the core iron density shows that it is changing significantly and its radiation is cooling the core electrons. Therefore we conclude that iron is playing a major role in this oscillation in contrast to carbon and oxygen whose radiation is oscillating only in reaction to the change in the edge electron temperature and density. The most likely candidate for the source of iron is the stainless steel divertor as this oscillation was only seen in experiments before the installation of carbon divertor tiles.

Acknowledgment

We would like to thank the member of LHD Experimental Groups 1 and 2 for their cooperation in

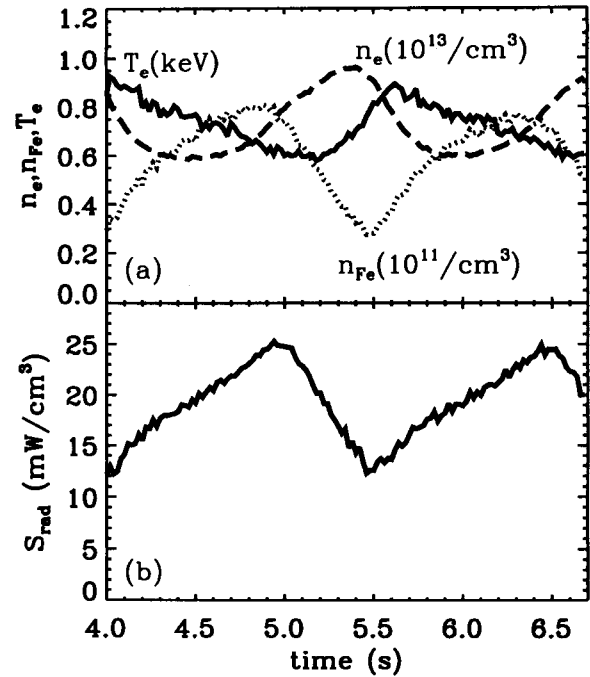


Fig. 6 Local parameters at $\rho = 0.4$ from shot 6690 (a) T_e , n_e , n_{Fe} and (b) S_{rad} .

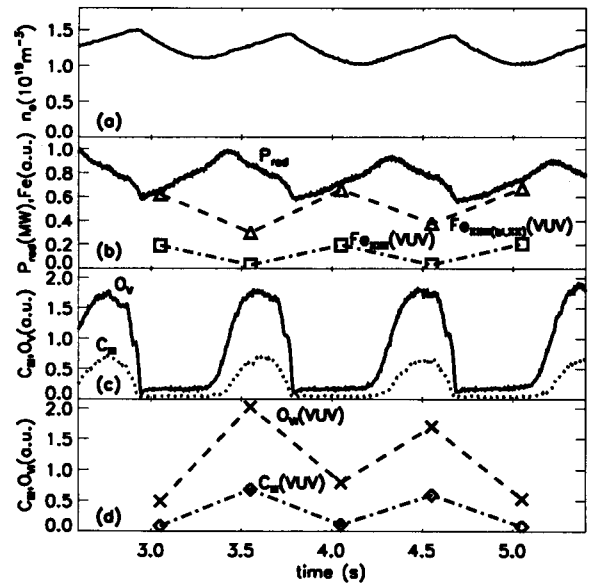


Fig. 7 Global parameters and spectroscopic signals from shot 6650.

performing the experiments.

References

[1] G. Fussman *et al.*, J. Nucl. Mater. **162**, 14 (1989).

- [2] R.J. Hawryluk *et al.*, Nucl. Fusion **19**, 1307 (1979).
- [3] K. Kondo *et al.*, J. Nucl. Mater. **196-198**, 303 (1992).
- [4] O. Motojima *et al.*, Phys. Plasmas **6**, 1843 (1999).
- [5] Y. Takeiri *et al.*, Plasma Phys. Control. Fusion, **42**, 147 (2000).
- [6] B.J. Peterson *et al.*, Proc. 26th EPS, Europhysics Conf. Absts. **23J**, 1337 (1999).
- [7] D.E. Post *et al.*, At. Data Nucl. Data Tables **20**, 397 (1977).
- [8] R.A. Hulse, Nucl. Tech./Fus. **3**, 259 (1983).
- [9] M.A. Graf, Ph. D. Diss., MIT (1995).
- [10] S. Morita and M. Goto, Ann. Report of National Inst. for Fusion Science, (1999) p. 151.